nature physics

LETTERS

PUBLISHED ONLINE: 3 APRIL 2011 | DOI: 10.1038/NPHYS1962

Tunable Kondo effect in graphene with defects

Jian-Hao Chen[1,2†], Liang Li[2], William G. Cullen[1,2], Ellen D. Williams[1,2] and Michael S. Fuhrer[1,2*]

Graphene is a model system for the study of electrons confined to a strictly two-dimensional layer[1] and a large number of electronic phenomena have been demonstrated in graphene, from the fractional[2,3] quantum Hall effect to superconductivity[4]. However, the coupling of conduction electrons to local magnetic moments[5,6], a central problem of condensed-matter physics, has not been realized in graphene, and, given carbon's lack of *d* or *f* electrons, magnetism in graphene would seem unlikely. Nonetheless, magnetism in graphitic carbon in the absence of transition-metal elements has been reported[7–9], with explanations ranging from lattice defects[10] to edge structures[11] to negative curvature regions of the graphene sheet[12]. Recent experiments suggest that correlated defects in highly-ordered pyrolytic graphite (HOPG), induced by proton irradiation[8] or native to grain boundaries[7], can give rise to ferromagnetism. Here we show that point defects (vacancies) in graphene[13] are local moments which interact strongly with the conduction electrons through the Kondo effect[6,14–16], providing strong evidence that defects in graphene are indeed magnetic. The Kondo temperature T_K is tunable with carrier density from 30 to 90 K; the high T_K is a direct consequence of strong coupling of defects to conduction electrons in a Dirac material[16].

We previously reported the resistivity of graphene with vacancies induced by ion irradiation in ultra-high vacuum (UHV; ref. 13). Here we present a detailed study of the gate voltage (V_g) and temperature (T) dependence of the resistivity $\rho(V_g, T)$ in similar graphene with vacancies over a wider temperature range 300 mK $< T <$ 290 K. Apart from weak-localization (WL) corrections[17,18], we find that $\rho(V_g, T)$ is explained by a temperature-independent contribution $\rho_c(V_g)$ due to non-magnetic disorder plus a temperature-dependent contribution $\rho_K(V_g, T)$, not present in as-prepared graphene[13], which follows the universal temperature dependence expected for Kondo scattering from a localized 1/2-spin with a single scaling parameter T_K.

Graphene with vacancies is prepared as described in ref. 13. After irradiation, the devices were annealed overnight at 490 K in UHV, and then exposed to air during transfer to a ^{3}He sample-in-vacuum cryostat. Figure 1a shows $\sigma(V_g)$ measured at 17 K for a graphene device (sample Q6) before irradiation, immediately after irradiation, and measured at 300 mK after annealing and transfer to the ^{3}He cryostat. V_g is applied to the Si substrate to tune the carrier density $n = c_g V_g/e$, where $c_g = 1.15 \times 10^{-8}$ F cm^{-2} is the gate capacitance, and e the elementary charge. The mobility of the device is approximately 4000, 300, and 2000 cm^2 V^{-1} s^{-1}, respectively, for these three measurements; the conductivity and mobility recover significantly after annealing and air exposure, consistent with our previous study[13]. From the post-annealing mobility we estimate that this device has a defect density, n_{imp}, of approximately 3×10^{11} cm^{-2}, although greater understanding of the effects of annealing and ambient exposure on vacancies in graphene is needed. See Supplementary Information for the calculation of defect density and also Raman spectra of the device before and after irradiation. Slight asymmetry between electron and hole conduction in the $\sigma(V_g)$ curve is also observed in the irradiated sample, which could indicate a non-zero on-site energy for the defects in graphene[19].

Figure 1b shows the perpendicular magnetic field dependence of the resistivity $\rho(B)$ of the irradiated sample Q6 at $T = 300$ mK at several different gate voltages. Negative magnetoresistance is observed at small B, indicating the dominance of weak localization arising from intervalley scattering due to lattice defects[17,18]. Figure 1c shows a detail of the magnetoresistance at small B, at 300 mK and at $V_g - V_{g,min} = -65$ V (see Supplementary Information for the gate voltage and temperature dependent phase coherence length, which is extracted from analyzing the WL magnetoresistance). Shubnikov–de Haas (SdH) oscillations appear at high B field. To measure the resistivity without WL and SdH corrections, the WL contribution is suppressed by application of $B = 1$ T in further measurements. For $|V_g - V_{g,min}| < 5$ V, SdH corrections may affect the data slightly at 1 T. However, as shown below, the $\rho(T)$ behaviour for $|V_g - V_{g,min}| > 5$ V and $|V_g - V_{g,min}| < 5$ V show no qualitative differences.

Figure 2a shows the temperature-dependent resistivity $\rho(T)$ of the irradiated graphene measured at several different gate voltages at $B = 1$ T. Positive slopes, $d\rho/dT > 0$, are seen in $\rho(T)$ from room temperature to about 200 K for V_g not too near $V_{g,min}$, indicating phonon contributions[20]; between ~10 and ~100 K, we find $d\rho/dT < 0$ and the resistivity increases logarithmically with decreasing temperature at all V_g. At low temperature the resistivity at all V_g saturates ($d\rho/dT \to 0$), indicating that there is no disorder-induced metal to insulator transition (MIT; ref. 16) or opening of a bandgap.

In metallic systems where localized magnetic moments couple anti-ferromagnetically to the conduction electrons, spin-flip scattering gives rise to an anomalous component of the resistivity $\rho_K(T)$ which is characterized by a Kondo temperature T_K (refs 6,21). For $T \approx T_K$, $\rho_K(T)$ is approximately logarithmic in T (similar behaviour is observed *in situ* in UHV before ambient exposure; see Supplementary Information). In principle, interaction effects in the presence of disorder could also lead to logarithmic $\rho(T)$ even at high magnetic field (the Altshuler–Aronov effect); however this would also lead to similar corrections to the Hall resistivity, which are not observed (see Supplementary Information). For $T \ll T_K$, the conduction electrons screen the spins of the local moments and the resistivity saturates, with a negative correction proportional to T^2 (ref. 22). To compare the observed data in graphene with vacancies to theories of the Kondo effect, we model the

[1]Materials Research Science and Engineering Center, University of Maryland, College Park, Maryland 20742, USA, [2]Center for Nanophysics and Advanced Materials, Department of Physics, University of Maryland, College Park, Maryland 20742, USA. †Present address: Department of Physics and Center of Integrated Nanomechanical Systems, University of California at Berkeley, Berkeley, California 94720, USA; Materials Sciences Division, Lawrence Berkeley National Laboratory, Berkeley, California 94720, USA. *e-mail: mfuhrer@umd.edu.

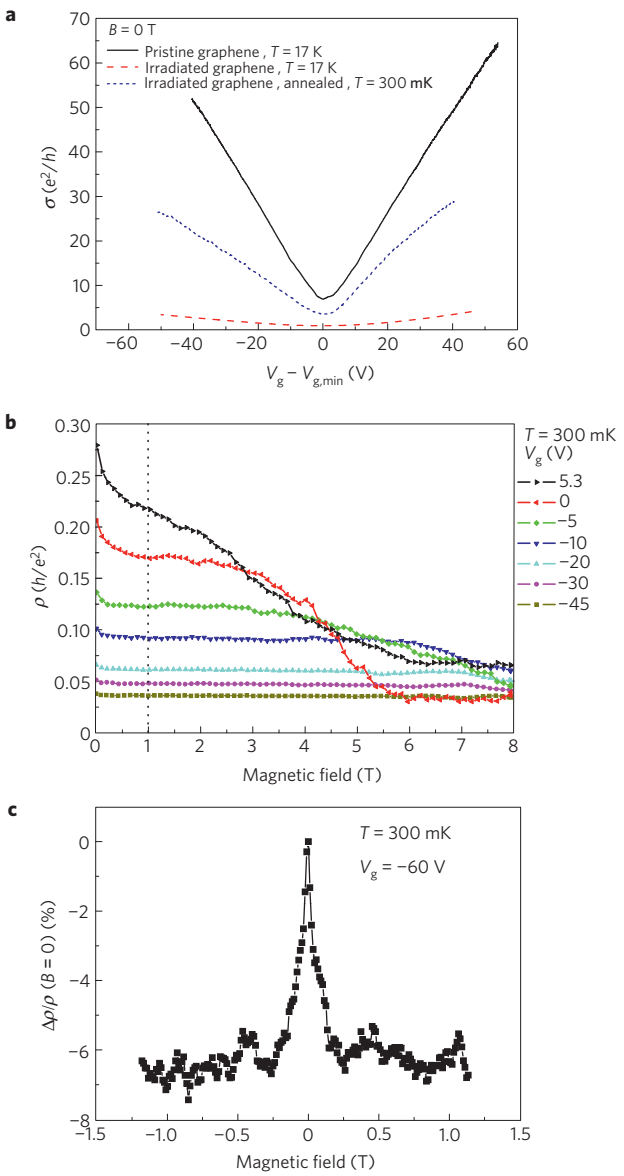

Figure 1 | Gate voltage dependent conductivity $\sigma(V_g)$ and magnetoresistance of the graphene sample. a, $\sigma(V_g)$ of the graphene sample Q6 before (black solid line) and after (red dashed line) irradiation with 500 eV He^+ at a temperature $T = 17$ K, and after annealing at 490 K overnight in ultra-high vacuum and exposure to ambient before cooling to $T = 300$ mK (blue short-dashed line). Magnetic field $B = 0$ for all data. The gate voltage of minimum conductivity $V_{g,min} = -8$ V, 5 V, 5.3 V for pristine, irradiated and annealed sample, respectively. **b**, Magnetoresistance of irradiated and annealed graphene sample for $B = 0$–8 T at various V_g. **c**, Normalized detailed magnetoresistance of irradiated and annealed graphene sample from −1.2 to 1.2 T at $V_g - V_{g,min} \approx -65$ V.

temperature-dependent resistivity in the low temperature regime and the intermediate temperature regime (region of maximum logarithmic slope, roughly between 10 and 100 K), respectively, as

$$\rho(V_g, T) = \rho_{c1}(V_g) + \rho_{K,0}(V_g)\left(1 - \left(\frac{\pi}{2}\right)^4 \left(\frac{T}{T_K(V_g)}\right)^2\right) \quad (1)$$

$$\rho(V_g, T) = \rho_{c2}(V_g) + \frac{\rho_{K,0}(V_g)}{2}\left(1 - 0.470 \ln\left(\frac{1.2T}{T_K(V_g)}\right)\right) \quad (2)$$

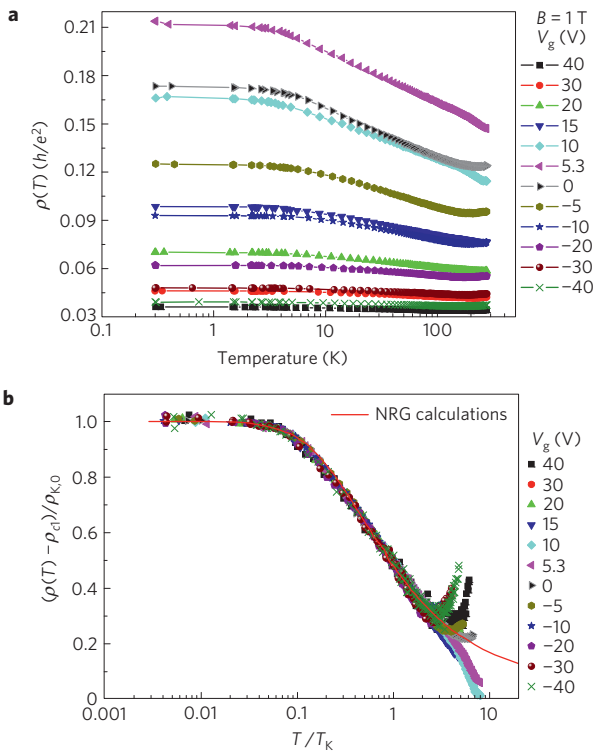

Figure 2 | Universal Kondo behaviour of graphene with defects. **a**, Temperature-dependent resistivity $\rho(V_g)$ of graphene sample Q6 under a perpendicular magnetic field of 1 T, at 12 different gate voltages, with temperature changing from 300 mK to ~290 K. **b**, The normalized Kondo part of the resistivity $(\rho - \rho_{c1})/\rho_{K,0}$ versus $T/T_K(V_g)$, where $T_K(V_g)$ is the Kondo temperature at respective gate voltage (see Fig. 4). The red line is the expected universal Kondo behaviour from numerical renormalization group calculations[21].

where $\rho_{K,0}$ is the Kondo resistivity at zero temperature, ρ_{c1} and ρ_{c2} the non-temperature-dependent part of the resistivity, presumably from impurity scattering that does not involve the spin degree of freedom[23,24]. The numerical factors in equations (1) and (2) are from the theory of the spin-1/2 Kondo effect[21]. As $\rho(V_g, T = 0)$ is known, there are three degrees of freedom in these equations at each V_g: ρ_{c1}, ρ_{c2} and T_K; if $\rho_K(T)$ follows the universal Kondo form then $\rho_{c1} = \rho_{c2}$. We keep ρ_{c1} and ρ_{c2} as independent parameters to test the internal consistency of the model. Least square fits to the equations (1) and (2) are carried out on $\rho(V_g, T)$ in the low and intermediate temperature ranges respectively (see Supplementary Information for details).

Using the extracted parameters, we can scale the $\rho(T)$ curves at different V_g and compare them to the universal Kondo behaviour[21,25]. Figure 2b shows the normalized Kondo resistivity $(\rho - \rho_{c1})/\rho_{K,0}$ versus T/T_K and the universal Kondo behaviour from numerical renormalization group calculations (NRG; ref. 21). From Fig. 2b one can find that: (1) all the experimental curves collapse to a single functional form for 300 mK $< T <\sim 3T_K$ and (2) the functional form matches well the universal Kondo behaviour from NRG calculations. At higher temperature ($T > 200$ K), phonon contributions become important[20] and the observed positive deviations from the NRG calculations are expected. However, at the lowest gate voltages, the deviation is negative, possibly due to thermal activation of carriers.

Now we discuss the gate voltage dependence of the extracted parameters, ρ_{c1}, ρ_{c2}, $\rho_{K,0}$ and T_K. Figure 3a shows ρ_{c1} and ρ_{c2} versus V_g, which peak around the actual minimum conductivity gate voltage $V_{g,min} \approx 5.3$ V. We find that ρ_{c1} and ρ_{c2} are practically

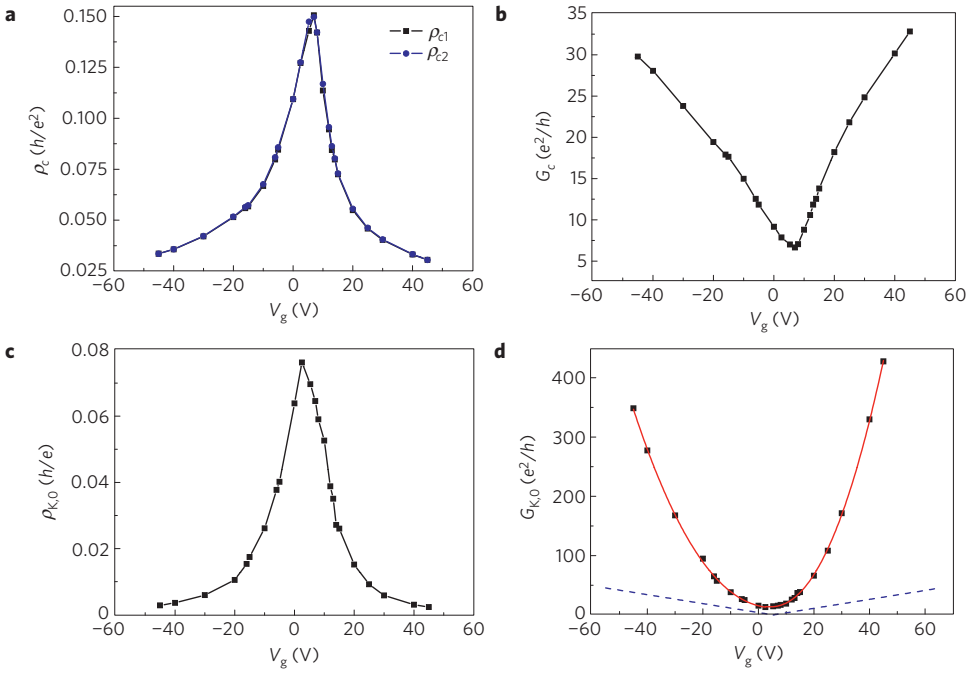

Figure 3 | The non-Kondo and Kondo part of the resistivity versus V_g. a, Comparison between the non-Kondo resistivity obtained from fitting $\rho(V_g, T)$ to equation (1) in the low temperature regime (ρ_{c1}) and to equation (2) in the intermediate temperature regime (ρ_{c2}) at different V_g. **b**, non-Kondo conductivity $G_c = 1/\rho_c$ as a function of V_g. **c**, The zero temperature Kondo resistivity $\rho_{K,0}$ and **d**, Kondo conductivity $G_{K,0} = 1/\rho_{K,0}$ as a function of V_g. The red solid line in **d** is a power law fit to $G_{K,0}, (V_g)$. The blue dashed line is the expectation for unitary scatterers of concentration 3×10^{11} cm^{-2} (ref. 15).

identical, which indicates that the logarithmic divergence and T^2 saturation of the resistivity indeed arise from the same effect (the Kondo effect). From now on we use ρ_{c1} for the non-Kondo resistivity and label it as ρ_c. Figure 3b shows the non-Kondo conductivity $G_c = 1/\rho_c$ as a function of V_g, which has a similar gate voltage dependence as an as-prepared graphene sample. That is linear $G(V_g)$ at high V_g, and a minimum G of a few e^2/h where h is Planck's constant. It is worth noting that the minimum non-Kondo conductivity $G_{c,\min} = 6.9e^2/h$ is the same as the minimum conductivity of the pristine sample before irradiation (see Fig. 1a).

Figure 3c shows the Kondo resistivity $\rho_{K,0} = \rho(T=0) - \rho_c$ versus V_g, which also peaks around the $V_{g,\min}$, and decreases rapidly with increasing $|V_g - V_{g,\min}|$, and Fig. 3d shows $G_{K,0} = 1/\rho_{K,0}$ versus V_g. In the low-temperature limit (saturated resistivity), we expect $G_{K,0} \approx (\pi e^2/h)(n/n_{imp})$ (ref. 15). However, $G_{K,0}$ is 3–10 times larger than expected for $n_{imp} = 3 \times 10^{11}$ cm^{-2}, and varies more rapidly; the red solid line is a power law fit to $G_{K,0}(V_g)$ that yields $G_{K,0} \sim A + BV_g^{\alpha}$, with $\alpha = 2.1 \pm 0.1$ for electron conduction and $\alpha = 2.2 \pm 0.2$ for hole conduction.

Figure 4 shows the gate voltage dependence of the Kondo temperature T_K. T_K is of order 50 K, which indicates strong coupling between the localized magnetic moment and the conduction electrons. Moreover, T_K is tunable by gate voltage, with a minimum of about 30 K near $V_{g,\min}$ and maxima close to 90 K at $V_g - V_{g,\min} \approx -20$ V (hole conduction) and close to 70 K at $V_g - V_{g,\min} \approx 25$ V (electron conduction). At higher gate voltages ($|V_g - V_{g,\min}| > 25$ V), T_K decreases slightly with gate voltage, although the experimental error becomes large at large V_g, as the Kondo resistivity become very small. T_K versus $V_g - V_{g,\min}$ for a second sample (sample L2, see Supplementary Information for details) shows similar magnitude and similar variation with gate voltage. The higher base measurement temperature (1.7 K for sample L2 as compare to 0.3 K for sample discussed in main text) results in larger uncertainty in T_K, and might result in a systematically smaller T_K obtained from the fitting. It is also possible that T_K depends on the initial

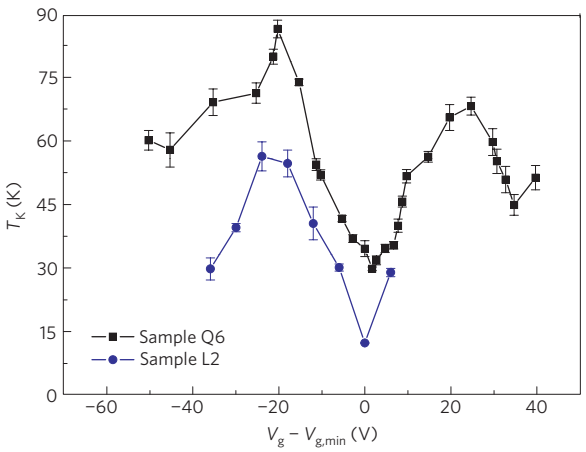

Figure 4 | The gate-tunable Kondo Temperature. The Kondo temperature T_K of two graphene samples with vacancies as a function of gate voltage V_g as determined from fits to equations (1) and (2). The sample Q6 (black squares) has been discussed in the main text. Details on sample L2 (blue circles) can be found in Supplementary Information. The error bars represent the ± one standard deviation of T_K, calculated using error propagation from the standard deviation of raw fitting parameters (see Supplementary Information).

disorder in the sample, as electron–hole puddling may play a role in determining T_K.

In a conventional (non-relativistic) Fermi liquid, we can roughly estimate the Kondo temperature:

$$k_B T_K \approx D e^{-1/J\rho(E_F)} \quad (3)$$

where k_B is Boltzmann's constant, D is the electronic bandwidth (~10 eV for π electrons in graphene), $J > 0$ the antiferromagnetic coupling constant, and $\rho(E_F) = 8\pi E_F/(h v_F)^2 = 4\sqrt{\pi n}/h v_F$ is the

density of states of graphene at the Fermi energy. Equation (3) predicts T_K vanishes exponentially as $E_F \to 0$. This is in contrast to the observed variation of only $\sim 3\times$ in T_K. The Kondo effect in a relativistic electron system is expected to differ qualitatively from the conventional non-relativistic Kondo effect[14,26,27]. In particular, for systems with $\rho(E_F) \propto |E_F|^r$, the case of $r = 1$ (expected for graphene) is critical, and T_K vanishes as $E_F \to 0$ either linearly or as a power law, depending on the sign of E_F. For $r > 1$, T_K remains finite, and for $r < 1$, T_K is exponentially suppressed, as $E_F \to 0$. A recent theoretical study[27] of (AB sublattice symmetric) Co on graphene found large T_K, of order 100 K, and strong asymmetry in T_K about $E_F = 0$, which we do not observe. However, the defects studied here are expected to break sublattice symmetry and locally open a gap at the Dirac point, with a sharp resonant midgap state leading to resonant impurity scattering as $E_F \to 0$ (refs 13,16). In this case, it has been pointed out that the dimensionless parameter which determines the strength of the Kondo effect, $J\rho(E_F)$ in equation (3), is proportional to the sine of the scattering phase shift for the defect, which for the large scalar potentials induced by defects in the graphene plane is finite and of order unity[16] as $E_F \to 0$, leading to a robust Kondo effect. For a resonant state located at exactly the Dirac point we would also expect a strong particle–hole asymmetry as the defect state is filled and emptied for positive or negative E_F. However, we suppose that a state located modestly below the Dirac point could be filled at all observable E_F (for $V_g < 50$ V, $E_F < 240$ meV) and still produce a strongly resonant scattering around $E_F = 0$ (ref. 19). It is also probable that in disordered graphene with potential fluctuations[28], the resistivity probes only the few defects with the largest T_K; this is consistent with $G_{K,0}$ larger than expected in the low-temperature limit (Fig. 3d). A complete theory of the Kondo effect in graphene will probably require both a microscopic understanding of the defect and its interaction with conduction electrons, as well as an effective medium theory of Kondo scattering in the presence of potential variations in disordered graphene.

The high T_K in graphene with its small density of states is a unique consequence of defect scattering in a Dirac system[16], and we anticipate that new graphene Kondo systems may be realized by a variety of physical or chemical modifications to the graphene lattice. Defect engineering thus provides a powerful route to introduce and control magnetism in carbon nanostructures, such as graphene and carbon nanotubes, without the presence of transition metal elements. The observation of Kondo scattering from defects in graphene may also explain the anomalous short spin lifetimes observed in graphene spin valves in the currently explored temperature range[29]; as a small native concentration of defects could be present in these (and perhaps all) graphene devices[30].

Received 29 April 2010; accepted 3 March 2011; published online 3 April 2011

References

1. Geim, A. K. Graphene: Status and prospects. *Science* **324,** 1530–1534 (2009).
2. Bolotin, K. I., Ghahari, F., Shulman, M. D., Stormer, H. L. & Kim, P. Observation of the fractional quantum Hall effect in graphene. *Nature* **462,** 196–199 (2009).
3. Du, X., Skachko, I., Duerr, F., Luican, A. & Andrei, E. Y. Fractional quantum Hall effect and insulating phase of Dirac electrons in graphene. *Nature* **462,** 192–195 (2009).
4. Heersche, H. B., Jarillo-Herrero, P., Oostinga, J. B., Vandersypen, L. M. K. & Morpurgo, A. F. Bipolar supercurrent in graphene. *Nature* **446,** 56–59 (2007).
5. Anderson, P. W. Localized magnetic states in metals. *Phys. Rev.* **124,** 41–53 (1961).
6. Kondo, J. Resistance minimum in dilute magnetic alloys. *Prog. Theor. Phys.* **32,** 37–49 (1964).
7. Cervenka, J., Katsnelson, M. I. & Flipse, C. F. J. Room-temperature ferromagnetism in graphite driven by two-dimensional networks of point defects. *Nature Phys.* **5,** 840–844 (2009).
8. Esquinazi, P. *et al.* Induced magnetic ordering by proton irradiation in graphite. *Phys. Rev. Lett.* **91,** 227201 (2003).
9. Ugeda, M. M., Brihuega, I., Guinea, F. & Gomez-Rodriguez, J. M. Missing atom as a source of carbon magnetism. *Phys. Rev. Lett.* **104,** 096804 (2010).
10. Lehtinen, P. O., Foster, A. S., Ma, Y., Krasheninnikov, A. V. & Nieminen, R. M. Irradiation-induced magnetism in graphite: A density functional study. *Phys. Rev. Lett.* **93,** 187202 (2004).
11. Fujita, M., Wakabayashi, K., Nakada, K. & Kusakabe, K. Peculiar localized state at zigzag graphite edge. *J. Phys. Soc. Jpn* **65,** 1920–1923 (1996).
12. Park, N. *et al.* Magnetism in all-carbon nanostructures with negative Gaussian curvature. *Phys. Rev. Lett.* **91,** 237204 (2003).
13. Chen, J-H., Cullen, W. G., Jang, C., Fuhrer, M. S. & Williams, E. D. Defect scattering in graphene. *Phys. Rev. Lett.* **102,** 236805 (2009).
14. Sengupta, K. & Baskaran, G. Tuning Kondo physics in graphene with gate voltage. *Phys. Rev. B* **77,** 045417 (2008).
15. Cornaglia, P. S., Usaj, G. & Balseiro, C. A. Localized spins on graphene. *Phys. Rev. Lett.* **102,** 046801 (2009).
16. Hentschel, M. & Guinea, F. Orthogonality catastrophe and Kondo effect in graphene. *Phys. Rev. B* **76,** 115407 (2007).
17. Morpurgo, A. F. & Guinea, F. Intervalley scattering, long-range disorder, and effective time-reversal symmetry breaking in graphene. *Phys. Rev. Lett.* **97,** 196804 (2006).
18. McCann, E. *et al.* Weak-localization magnetoresistance and valley symmetry in graphene. *Phys. Rev. Lett.* **97,** 146805 (2006).
19. Wehling, T. O., Yuan, S., Lichtenstein, A. I., Geim, A. K. & Katsnelson, M. I. Resonant scattering by realistic impurities in graphene. *Phys. Rev. Lett.* **105,** 056802 (2010).
20. Chen, J-H., Jang, C., Xiao, S., Ishigami, M. & Fuhrer, M. S. Intrinsic and extrinsic performance limits of graphene devices on SiO2. *Nature Nanotech.* **3,** 206–209 (2008).
21. Costi, T. A. *et al.* Transport coefficients of the Anderson model via the numerical renormalization group. *J. Phys. Condens. Matter* **6,** 2519–2558 (1994).
22. Nozières, P. A Fermi-liquid description of the Kondo problem at low temperatures. *J. Low Temp. Phys.* **17,** 31–42 (1974).
23. Chen, J-H. *et al.* Charged impurity scattering in graphene. *Nature Phys.* **4,** 377–381 (2008).
24. Jang, C. *et al.* Tuning the effective fine structure constant in graphene: Opposing effects of dielectric screening on short- and long-range potential scattering. *Phys. Rev. Lett.* **101,** 146805 (2008).
25. Goldhaber-Gordon, D. *et al.* From the Kondo regime to the mixed-valence regime in a single-electron transistor. *Phys. Rev. Lett.* **81,** 5225–5228 (1998).
26. Cassanello, C. R. & Fradkin, E. Kondo effect in flux phases. *Phys. Rev. B* **53,** 15079–15094 (1996).
27. Vojta, M., Fritz, L. & Bulla, R. Gate-controlled Kondo screening in graphene: Quantum criticality and electron-hole asymmetry. *Europhys. Lett.* **90,** 27006 (2010).
28. Rossi, E. & Das Sarma, S. Ground state of graphene in the presence of random charged impurities. *Phys. Rev. Lett.* **101,** 166803 (2008).
29. Popinciuc, M. *et al.* Electronic spin transport in graphene field-effect transistors. *Phys. Rev. B* **80,** 214427 (2009).
30. Ni, Z. H. *et al.* On resonant scatterers as a factor limiting carrier mobility in graphene. *Nano Lett.* **10,** 3868–3872 (2010).

Acknowledgements

This work has been supported by NSF-UMD-MRSEC grant DMR 05-20471 (J-H.C., W.G.C., E.D.W., M.S.F.) and the US ONR grant N000140610882 (W.G.C., E.D.W., M.S.F.). The MRSEC SEFs were used in this work. Infrastructure support has also been provided by the UMD NanoCenter and CNAM. We would also like to thank D. Goldhaber-Gordon, S. D. Sarma, E. Rossi, E. Hwang and J. Zhu for useful discussions.

Author contributions

J-H.C. and M.S.F. conceived the experiments, J-H.C. and L.L. fabricated devices, J-H.C. performed the experiments and analyzed the data, J-H.C., W.G.C., E.D.W. and M.S.F. co-wrote the paper. All authors discussed the results and commented on the manuscript.

Additional information

The authors declare no competing financial interests. Supplementary information accompanies this paper on www.nature.com/naturephysics. Reprints and permissions information is available online at http://npg.nature.com/reprintsandpermissions. Correspondence and requests for materials should be addressed to M.S.F.